# Deforestation Projections for Carbon-Rich Peat Swamp Forests of Central Kalimantan, Indonesia

**ARTICLE** *in* ENVIRONMENTAL MANAGEMENT · FEBRUARY 2011

Impact Factor: 1.72 · DOI: 10.1007/s00267-011-9643-2 · Source: PubMed



**3 AUTHORS:**


Douglas O Fuller
University of Miami


Martin Hardiono



Erik Meijaard
Borneo Futures, Brunei

Environmental Management (2011) 48:436–447
DOI 10.1007/s00267-011-9643-2

# Deforestation Projections for Carbon-Rich Peat Swamp Forests of Central Kalimantan, Indonesia

Douglas O. Fuller · Martin Hardiono · Erik Meijaard

Received: 10 June 2010 / Accepted: 4 February 2011 / Published online: 27 February 2011


**Abstract** We evaluated three spatially explicit land use and cover change (LUCC) models to project deforestation from 2005–2020 in the carbon-rich peat swamp forests (PSF) of Central Kalimantan, Indonesia. Such models are increasingly used to evaluate the impact of deforestation on carbon fluxes between the biosphere and the atmosphere. We considered both business-as-usual (BAU) and a forest protection scenario to evaluate each model's accuracy, sensitivity, and total projected deforestation and landscape-level fragmentation patterns. The three models, Dinamica EGO (DE), GEOMOD and the Land Change Modeler (LCM), projected similar total deforestation amounts by 2020 with a mean of 1.01 million ha (Mha) and standard deviation of 0.17 Mha. The inclusion of a 0.54 Mha strict protected area in the LCM simulations reduced projected loss to 0.77 Mha over 15 years. Calibrated parameterizations of the models using nearly identical input drivers produced very different landscape properties, as measured by the number of forest patches, mean patch area, contagion, and Euclidean nearest neighbor determined using Fragstats software. The average BAU outputs of the models suggests that Central Kalimantan may lose slightly less than half (45.1%) of its 2005 PSF by 2020 if measures are not taken to reduce deforestation there. The relatively small reduction of 0.24 Mha in deforestation found in the 0.54 Mha protection scenario suggests that these models can identify potential leakage effects in which deforestation is forced to occur elsewhere in response to a policy intervention.

**Keywords** LUCC models · Terrestrial carbon · Deforestation · Indonesia · Peat swamp forest · Landscape metrics

D. O. Fuller (✉)
Department of Geography and Regional Studies,
1000 Memorial Drive, University of Miami, Coral Gables,
Florida 33124-2221, USA
e-mail: dofuller@miami.edu

M. Hardiono
Jl. Bukit Nusa Indah, No. 70, Ciputat, 15414 Jakarta, Indonesia
e-mail: martin.hardiono@gmail.com

E. Meijaard
People & Nature Consulting International, Vila Lumbung House
No. 6, Jalan Raya Petitenget 1000X, Kerobokan, Badung,
80361 Bali, Indonesia

## Introduction

Over the past twenty years, Indonesia's forests have declined dramatically in extent through a sequence of unsustainable logging practices, fires and plantation development (Murdiyarso and Lebel 2007; Curran and others 2004; Fuller and others 2004; Hansen and others 2009). Deforestation has been particularly intense throughout Sumatra and Indonesian Borneo (Kalimantan), which were once dominated by vast dipterocarp forests of exceptional biological diversity and high timber value (Whitten and others 1987; MacKinnon and others 1996). More recently, as lowland dipterocarp forests on mineral soils have become increasingly degraded and converted to plantations (Dennis and Colfer 2006; Langner and Siegert 2009), development of peat swamp forests (PSF) has accelerated. Because these peats are very carbon-rich, concerns have grown over massive emissions of carbon dioxide released through burning and oxidation of PSF biomass and peat soils (Page and others 2002; van der Werf and others 2008). Kalimantan still contains a large amount of PSF, which typically is found in low-lying areas on waterlogged, anaerobic soils of relatively low pH. High amounts of soil organic carbon tend to accumulate under such conditions, unless peat soils are disturbed through drainage, logging and fire (Page and others 2009).

Estimates of Indonesia's mean annual carbon emissions between 2000 and 2004 vary from 1.66 to 2.40 Gigatonnes (Gt) with uncertainty owing to emissions from land use and cover change (LUCC) and peat fires. Approximately two thirds of these emissions come from LUCC rather than combustion of fossil fuels (Government of Indonesia 2009). Recurrent fires and deforestation on the islands of Borneo and Sumatra (van der Werf and others 2008) account for over 96% of fire-related emissions in equatorial Asia and over half of Indonesia's carbon emissions (Government of Indonesia 2009). Moreover, the carbon stored in tropical peat soils such as those found in Indonesia can exceed 18 times the carbon content of undisturbed forest vegetation above peat (Jaenicke and others 2008). The burning of peat soils and biomass in the province of Central Kalimantan during the severe El Niño fires of 1997 produced an estimated 0.19–0.23 Gt C flux to the atmosphere (Page and others 2002). The PSF of this Indonesian province is among the most extensive in Asia and contains an estimated total carbon store of 2.82–5.40 Gt (Page and others 2002). Since the El Niño fires of 1997, PSF in Central Kalimantan has been extensively converted and drained for plantation agriculture and further degraded by logging (Ballhorn and others 2009; Page and others 2009). Therefore, mitigation efforts such as avoided deforestation, fire suppression, re-wetting of peatland and PSF restoration have been identified as ways to reduce high carbon emissions from these ecosystems (Page and others 2009).

Spatial data obtained from the Indonesian Ministry of Forestry (MoF) indicated that Central Kalimantan lost approximately 0.84 Mha of peat swamp forest between 1995–2005, with much of this loss concentrated in the now-abandoned Mega Rice Project (MRP), which was intended to drain and clear nearly a million ha of peatland for (ultimately unsuccessful) rice cultivation. Reducing carbon emissions from deforestation and forest degradation (REDD) from such large-scale conversions requires reliable estimates of emissions levels using business-as-usual (BAU) scenarios against which mitigation measures such as forest protection and restoration can be measured (Olander and others 2008; Busch and others 2009; Obersteiner and others 2009). An important first step to develop BAU scenarios is application of LUCC models that can project the potential amount of change in forest area through time (Gibbs and others 2007; Harris and others 2008).

Here, we model PSF deforestation based on recent deforestation estimates obtained from comparison of Government of Indonesia (GoI) land cover maps (Fig. 1). Since spatial data on forest degradation are lacking for most of Indonesia, including Central Kalimantan, we did not consider forest degradation in our analysis. The spatially explicit LUCC models included Dinamica EGO (DE), GEOMOD and the Land Change Modeler (LCM). Each model uses a set of spatial data layers related to proximate deforestation drivers (sensu Geist and Lambin 2002) such as rivers, roads, fires, markets, settlements, etc., and thus can be parameterized with a common set of layers, which facilitates comparison and analysis of model outputs. Below we refer to this type of model as *proximate driver LUCC models* to distinguish them from other LUCC models such as agent-based models, which are generally based on interviews with agents of change and attempt to model decisions often made at the household level (e.g., Deadman and others 2004; Pontius and others 2007). The proximate driver LUCC models we selected for our analysis use similar methods and raster data structures but provide different levels of sophistication and flexibility for projecting land cover change. We selected 2020 as the endpoint of our simulations to coincide with Government of Indonesia's pledge to reduce $CO_2$ emissions relative to 2005 levels by 0.78 Gt over the next decade (Government of Indonesia 2009). Overall, the major aims of our analysis were: (1) to conduct LUCC model evaluation, validation and sensitivity analysis, (2) to investigate a range of potential PSF deforestation scenarios over a fifteen year horizon (i.e., primarily the quantity of change as well as potential allocation of change), and (3) to assess the potential effects of a major conservation and REDD intervention (establishment of a large protected area) on projected PSF deforestation.

## Materials and Methods

### Data Selection and Processing

As the basis of our forest change analysis we utilized two digital land cover maps for 1995 and 2005 (unpublished) of Central Kalimantan from GoI sources that were derived from interpretation of 30 m Landsat imagery. From each of these maps, we extracted the PSF class and reclassified all other classes to "other land" to create Boolean land cover maps representing the distribution of PSF in 1995 and 2005 (Fig. 1). These maps were then gridded to 500 m resolution to match the resolution of the driver layers. We lacked information to assess the accuracy of the 1995 PSF distribution; however, we performed qualitative (i.e., visual) assessment of the 2005 PSF map by comparing it with a 2006 Landsat-5 TM image (path 118, row 62), which suggested good agreement between 30 m imagery and 2005 PSF distribution.

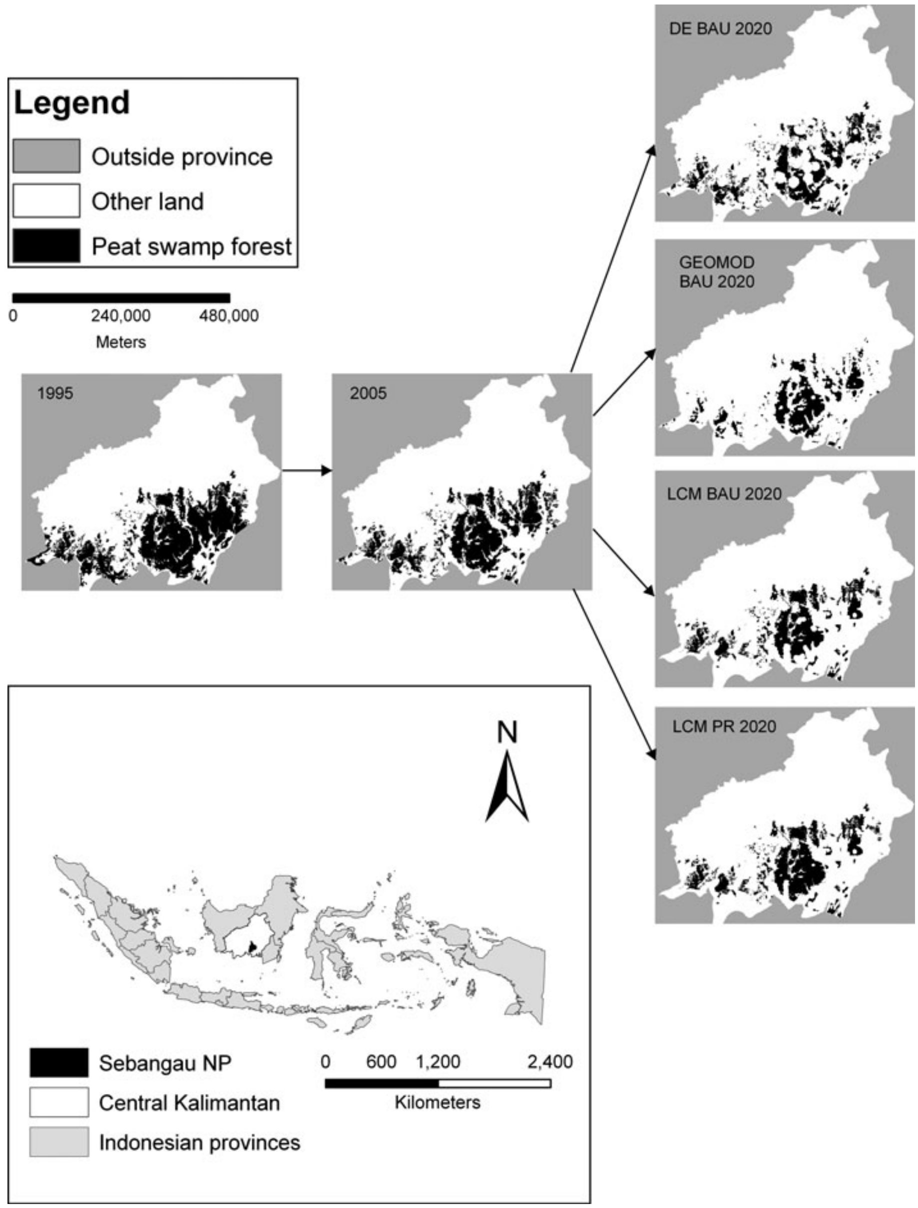


**Fig. 1** Peat swamp forest in 1995, 2005 and future projections using a business-as-usual (*BAU*) and a protection (*PR*) deforestation scenarios from GEOMOD, Dinamica EGO (*DE*) and the Land Change Modeler (*LCM*) for calibrated/validated model runs through 2020. The *black areas* in the 1995, 2005 and 2020 *panels* show areas of peat swamp forest (*PSF*) and the *inset* on the *bottom left* shows the general location of the study area as well as Sebangau National Park (*NP*)

The model driver data sets were obtained from the Indonesia-Australia Forest Climate Partnership (IACFP) office in Palangkaraya, Central Kalimantan. These data sets are given in Table 1 and included five key spatial data layers (proximate drivers) generally associated with tropical deforestation (Geist and Lambin 2002): active fire locations (hotspots) derived from the Advanced Very High Resolution Radiometer (AVHRR) from 1997, 2005–2006 hotpots from the Moderate Resolution Imaging Spectrometer (MODIS collection 4), and a map of rivers. Hotspots from 1997 and 2005–2006 were used because these coincided most closely to the dates of the land cover maps, hotspots maps were unavailable before the major El Niño event of 1997–1998, and this event was associated with a large amount of deforestation (Fuller 2003; Fuller and others 2004). The roads layer was derived from on-screen digitization of interpreted Landsat ETM + imagery from 1999–2003. Although we treat this layer as static, we recognize that changes in road infrastructure are expected from 2004–2020, and that the quantity and allocation of these changes are difficult to predict. Each layer was gridded to a 500 m resolution, assigned a common projection and coordinate system (UTM zone 50 south) and converted to distance layers using GIS software where each raster cell represents the distance in meters from the discrete feature of interest (i.e., distance from roads, distance from rivers, distance from AVHRR hotspots 1997, distance from MODIS hotspots 2005–2006, and distance from prior PSF deforestation locations derived from overlay of 1995 and 2005 PSF distributions).

Table 1 Model details for 11/41 validation runs that represent the full range of values obtained from the figure of merit in our study

| Model run | Description | Driver inputs | Key parameters |
|---|---|---|---|
| DE five statics | DE run using five input layers-BAU | Distance from: roads, rivers, hotspots (1997, 2005–2006), past deforestation | Transition probability matrix determined from overlay of 1995 and 2005 land cover maps |
| DE naïve | DE run with only one driver layer-BAU | Distance from past deforestation | Same as above |
| DE no roads | DE run with four input layers, key roads layer excluded-BAU | Distance from: rivers, hotspots (1997, 2005–2006), past deforestation | Same as above |
| GEOMOD 3 × 3 four statics | GEOMOD run with four layers-BAU | Distance from: roads, rivers, hotspots (1997), and past deforestation | Deforestation quantity from linear extrapolation from past rates; model run with the 3 × 3 window constraint, which limits change to forest edge locations; driver weights equal. |
| GEOMOD four statics unconstrained (uncon) | GEOMOD run with four layers-BAU | Same as above | Same as above but without the 3 × 3 window constraint |
| GEOMOD 3 × 3 naïve | GEOMOD run with four layers-BAU | Distance from past deforestation only | Same as GEOMOD 3 × 3 four statics |
| GEOMOD no roads | GEOMOD run with three layers-BAU | Distance from: rivers, hotspots, and past deforestation | Same as GEOMOD 3 × 3 with four statics |
| LCM five statics | LCM run with five static layers-BAU | Distance from: roads, rivers, hotspots (1997, 2005–2006), and past deforestation | Transition probabilities determined the same as DE five statics |
| LCM naïve | LCM run with one layer-BAU | Distance from past deforestation | Same as above |
| LCM(PR) | Protection or leakage scenario that restricts simulated deforestation to areas outside the Sebangau National Park, run with five static layers | Same as LCM five statics | Same as above |
| LCM no roads | LCM run with four static layers | Distance from: rivers, hotspots (1997, 2005–2006), and past deforestation | Same as above |

## Model Description and Application

The three models (DE, GEOMOD and the LCM) simulate land cover change using a multi-step parameterization process. Each can employ a cellular automaton that considers neighboring cell states at each time step. The DE and LCM utilize Markov transition probabilities derived from overlay of land cover maps representing the landscape at two points in time and spatially explicit (i.e., per cell) transition potentials that are scaled in various ways. As we simulated only the transition from forest to non-forest, the use of a Markov transition probability matrix is equivalent to an exponential decay of forest. DE uses a Bayesian Weights of Evidence method in which the effect of each spatial variable on a transition is calculated independently (Soares-Filho and others 2009).

The LCM uses either back-propagation neural network or logistic regression to combine spatial variables and to create a transition potential surface for each land cover transition (Eastman 2006). LCM establishes the quantity of change by evaluating the empirical Markov matrix based on comparison between the initial and second forest cover maps in time and then assumes this same transition probability as it projects into the future. The LCM allows users to vary the transition probabilities and we modified the transition probabilities for a set of LCM runs to examine how increasing the probability of deforestation would change spatial allocation. For our LCM simulations, we selected the neural network approach based on prior experience (Fuller 2005) with this particular algorithm. As cross-tabulation of the 1995 and 2005 maps indicated no transition from non-PSF to PSF (i.e., forest regeneration), although the LCM provides this possibility in cases where transitions between forest and non-forest are bidirectional.

GEOMOD does not use a Markov Chain approach but instead projects LUCC forward in time from an initial land cover map, a scaled suitability image derived from a weighted linear combination of driver variables (Pontius and others 2001). GEOMOD does not simulate quantity of change, but instead simulates the spatial allocation of forest change and the user must specify the projected areal change from data outside the model, which we derived using a linear extrapolation from historical deforestation rates from 1995–2005.

The specific steps used to parameterize the DE involved: (1) Determination of the transition probability matrix; (2) Determination of weights of evidence ranges; (3) Calculation of weights of evidence coefficients; (4) Determination of likely patch size configuration based on mean and variance of PSF patch size in the 2005 map and an estimated 50% reduction in patch area and doubling of patch size variance by 2020; (5) Creation of a model script that specifies the number of iterations and incorporates steps 1-4 above. We also varied the mean and variance of the patch size to examine how this parameter affected the projected 2009 deforestation.

For GEOMOD validations we also varied the neighborhood constraint, which is based on a nearest neighbor principle, in which an algorithm restricts land change within any one time step to cells that are on the edge of forested and non-forested pixels. This rule simulates the manner in which new deforestation can grow out of previous deforestation (Pontius and Chen 2006). In addition, we varied the number of cells expected to transition from PSF to non-PSF at each time step from 2006–2009. Consistent with guidelines offered in Pontius and Chen (2006) we did not include 2005–2006 MODIS fire observations as part of the GEOMOD simulations as including a future driver would violate the assumptions of the model. We also ran the model using the unconstrained option with four static, distance-based driver layers with equal weights applied to each layer, which was done because we possessed no a priori knowledge about which drivers may be most important. For this particular model run, we also assumed a linear extrapolation of forest loss from cross-tabulation of the 1995–2005 PSF maps.

Because the LCM allows for broad flexibility for planning infrastructure changes, conservation planning, and multiple transitions among different classes, and produced relatively high accuracy in the 2009 simulation (see section below), we utilized this model for the protection (PR) scenario in which the effects of this major policy intervention were considered at each time step. As this type of scenario must allocate a specified quantity of change in space, some authors refer to this type of simulation as a "leakage" scenario, which is a term used to describe a spatial shift of deforestation activities in response to a policy intervention such as improved enforcement of existing laws or changes in land-use designation (Pontius and others 2009). The PR scenario was initiated when the 0.54 Mha Sebangau National Park (Fig. 1) was established in 2006; the model assumed that no deforestation could take place within the protected area.

We projected deforestation from 2005–2020 using three business-as-usual (BAU) and one protection (PR) scenario to generate a range of potential deforestation estimates. Consistent with other studies (Siegert and others 2001; Murdiyarso and Lebel 2007; Dennis and Colfer 2006) we also assumed that fire is associated with deforestation and leads to eventual, complete loss of above-ground woody biomass. To evaluate each model's sensitivity, we varied the number of input layers by incorporating different driver layers as follows: a complete set of five spatial distance drivers treated as static components over the simulation period ("five statics"); three distance-based layers including roads, rivers and distance from past deforestation ("no fire"); the five statics minus roads ("no roads"); five statics minus rivers ("no rivers") and distance from past deforestation only ("naïve model").

A subset of three simulated landscape time series was then evaluated using Fragstats, a standard tool for quantifying landscape-level spatial patterns that provides numerous landscape metrics relating to the spatial configuration such as dispersion, clumping, connectivity, interspersion, patch isolation, and patch shape (McGarigal and Marks 1995). To simplify the analysis, we selected three of four sets of simulations, DE (BAU), GEOMOD $3 \times 3$ (BAU), LCM (BAU), LCM (PR), which represented a wide range of projected deforestation quantities. We selected four commonly used, simple metrics to assess different spatial aspects of the simulated landscapes: number of patches, mean patch area, contagion (a measure of dispersion or clumping), and Euclidean nearest neighbor (a measure of connectivity) (Li and others 2005).

## Model Validation

The LUCC models were parameterized using these distance-based layers simulations to generate a total of 41 projected 2009 PSF/non-PSF maps for subsequent validation. These 41 runs represent a wide range of different parameterizations, which of course may involve unlimited combinations of different parameter values and inputs, but for practical purposes we limited the scope of analysis to the major types of variations possible for each of the models as described in the section above. Each of the 41 validation runs was assessed against a set of reference polygons digitized from visual interpretation of two 2009

Landsat ETM + images (Path 116, Row 61 and Path 116, Row 62 acquired on 6 and 22 May 2009, respectively), which covered approximately 30% of the entire study area. These images were selected because they contained less than 50% cloud cover and were freely available from the US Geological Survey site (http://glovis.usgs.gov/). Mature PSF was clearly distinguishable in 30 m Landsat ETM + color composites as areas of forest with homogeneous texture relative to forests on mineral soils. PSF and non-PSF polygons were also overlaid and compared to the GoI maps to provide an additional qualitative assessment of accuracy. A reference sample was taken owing to partial cloud cover and missing data values in the 2009 ETM + scan-line corrector off (SLC-off) images. Each reference polygon was labeled as either PSF or non-PSF land cover and spatial allocation of 2009 LUCC simulations was assessed using the figure-of-merit statistic, which ranges from 0% for no agreement between simulated parameters and reference data to 100% for perfect agreement. The figure of merit is a statistical measurement, which is expressed as the ratio of the intersection of the observed change and simulated change to the union of the observed and predicted change (Pontius and others 2008).

Validation data development resulted in 152,075 ha sample of clearly distinguishable PSF and non-PSF forest locations with 2,687 PSF cells and 3,396 non-PSF cells. Of these cells, 2,659 remained in the non-PSF category from 2005–2009, 737 changed from PSF to non-PSF, 17 changed from non-PSF to PSF and 2,670 remained in the PSF category. The models were calibrated so that the combination of model parameters that produced the most accurate simulations for 2009 were retained for the deforestation simulations over the 2005–2020 period. Figure 2 shows the figures of merit for 11 of the 41 runs, which were selected because they reveal the full range of values obtained for this metric; Table 1 provides more details on these particular model runs.

## Results

Figure 2 shows that the figure of merit, which can be interpreted readily as the length of the cross-hatched segment divided by the length of the entire bar for each model run, ranged from 27% for the LCM without roads to less than one percent for the GEOMOD parameterization that was unconstrained by a neighborhood window. It also shows that the naïve models produced comparable values relative to parameterizations that included three more drivers (Fig. 2). Overall, the median value for the figure of merit for 41 validation runs was 17 percent. Fig. 2 shows that nearly all of the model runs have a quantity of deforestation that is less than half of the quantity of deforestation in the validation data. The 2009 validation indicates that 12% of the landscape experienced deforestation, while 10 of the 11 model runs show predictions that have less than 6% deforestation

In the case of the LCM, removal of the roads layer as one of the drivers increased the figure of merit, which suggests that the inclusion of additional drivers may not provide more accurate simulations of deforestation than predictions based solely on distance from past deforestation. Further, if the error from observed change predicted as persistence shown as the black segment (i.e., omissions

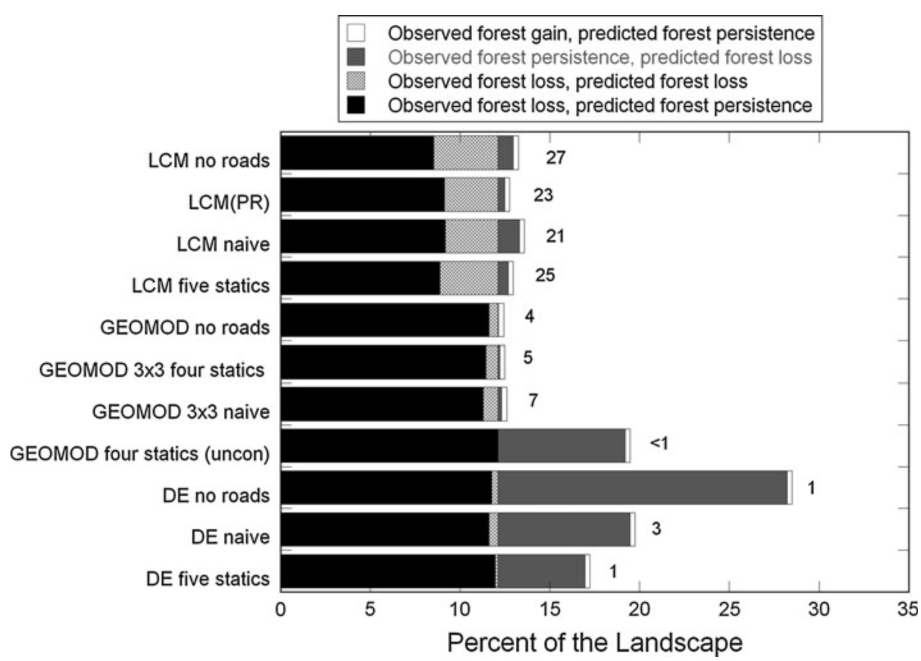


**Fig. 2** The figure of merit shown for 11/41 model validation runs. The FM is the length of the crosshatched segment divided by the total length of each bar, where 100% is perfect agreement and zero is no agreement. The value at the end of each bar gives the figure of merit in percent for each of the 11 model runs

or misses) is roughly equal to the error from observed persistence predicted as change as the solid gray segment (commissions or false alarms), then the overall quantity error is low relative to the error due to spatial allocation. This was the case for DE no roads, DE naive, and GEOMOD four statics unconstrained, which suggests that these model runs may be particularly good at projecting future change quantities. For example, the GEOMOD four statics unconstrained run predicted 68,547 ha of remaining PSF and 83,578 ha of non-PSF in 2009, while the 2009 validation polygons contained 67,197 ha and 84,928 ha of PSF and non-PSF, respectively. The DE with five statics, GEOMOD 3 × 3 constrained, and LCM with five statics over-predicted the amount of remaining PSF by 17,928, 16,856 and 16,706 ha, respectively. This also means that these runs under-predicted the amount of non-PSF by varying amounts ranging from 17,978 ha for DE with five statics to 16,706 ha for LCM with five statics. Moreover, the relatively high figures of merit (>20%) for the LCM validation runs suggest that these model parameterizations may be most appropriate for simulating future spatial allocation of change. It should be noted that the white segment that shows the error from observed change as wrong gaining category (i.e., apparent reforestation or forest regrowth) was constant among the simulations. This is due to a 17-cell disagreement between the 2009 validation polygons that showed forest, whereas the 2005 map displayed non-forest at these locations. This error may relate to either misinterpretation of the Landsat ETM + imagery or, more likely, the 2005 map itself, which may have omitted some areas of PSF. Of course, it is also possible that a modest amount of forest regrowth actually occurred from 2005–2009.

GEOMOD 3 × 3 BAU shows the assumed linear accumulation of forest loss (Fig. 3), whereas the two other models reflect the curves that the Markov assumptions imply. The LCM and DE simulations produced nearly identical deforestation curves, which show that although the two models implement LUCC modeling differently, their underlying approaches result in similar change quantities, but not necessarily change locations. DE and LCM models projected similar total deforestation amounts (0.90 Mha, 0.91 Mha) by 2020; whereas GEOMOD 3 × 3 projected 1.27 Mha of forest loss by 2020 (Fig. 3). Further, inclusion of the 0.54 Mha Sebangau NP in the LCM BAU limited the loss to 0.77 Mha by 2020. The 2020 BAU mean of the three models was 1.01 Mha (standard deviation or s.d. = 0.17 Mha), which equates to a deforestation rate of 2.6%/year and is similar to what Achard and others (2002) found for deforestation rates in Southeast Asia from 1990–1997. In other words, the average output of the models suggests that Central Kalimantan may lose slightly less than half (45.1%) of its 2005 PSF if measures are not

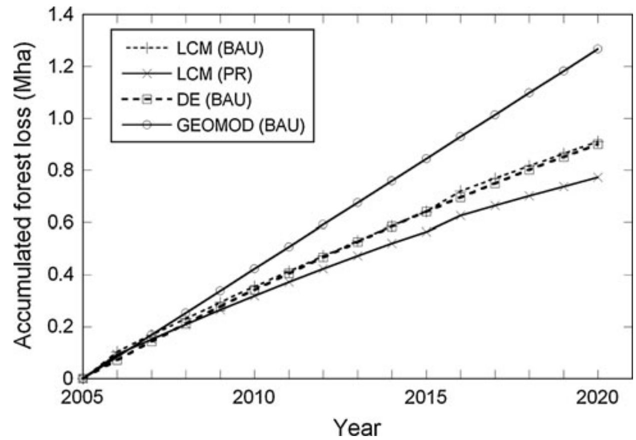


**Fig. 3** Deforestation time series projected using the three *LUCC* models and two different scenarios, business as usual (*BAU*) and protection (*PR*). The BAU projections are LCM with five static drivers, DE with five statics, GEOMOD with four static drivers and the 3 × 3 window constraint, and GEOMOD with four static drivers and no window constraint. More details on the model parameters can be found in Table 1

taken to reduce deforestation there. The relatively small reduction of 0.24 Mha in deforestation from the LCM PR simulation relative to the three-model BAU mean of 1.01 Mha suggests that the LCM indirectly simulates potential leakage effects in which agents of deforestation shift their activities to other areas as a response to the establishment of a strict protected area. However, it must be borne in mind that this leakage scenario results from the model's attempt to allocate deforestation and is not based on the decision behavior of any agents per se.

BAU projections shown in Fig. 3 reveal increasing divergence between GEOMOD and the other three projections by 2009. Overall, the GEOMOD 3 × 3 BAU simulation produced a highly compact spatial pattern of remnant PSF forest patches, with only 188 unique (non-contiguous), large patches having a mean area of 7,414 ha (Figs. 3, 4a). The 2020 DE BAU simulation produced a landscape with 620 PSF unique patches with a mean patch size of 2,838 ha, while the 2020 LCM BAU simulation resulted in 865 unique patches with a mean patch size of 4,877 ha. These landscape metrics indicate that over the 15-year modeling horizon DE and the LCM produced more diffuse, and thus fragmented spatial patterns relative to GEOMOD.

To assess the overall spatial similarity among the three main 2020 BAU projections, we performed pair-wise comparisons by calculating the percent agreement from the error matrix between maps. Percent agreement is scaled from zero, indicating no spatial agreement, to 100 for maps that show perfect agreement. The percent agreement for the 2020 DE and GEOMOD simulations was 90.16; whereas the comparison for the 2020 DE and LCM simulations

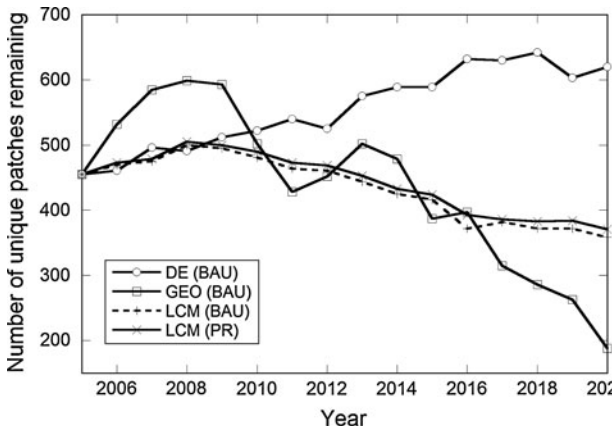


**Fig. 4** Number of unique forest patches remaining through 2020 simulated using the three LUCC models and two different scenarios

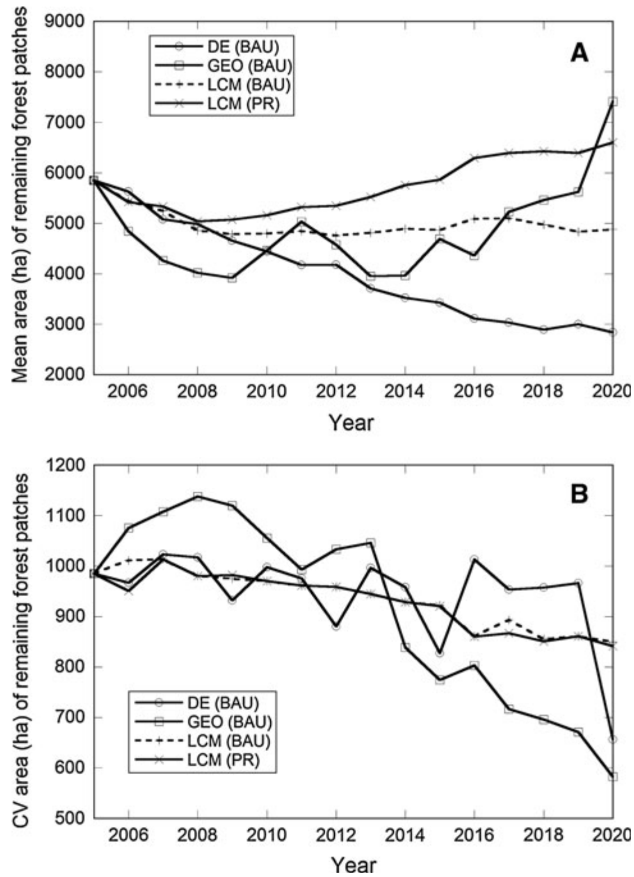


**Fig. 5** **a** Mean area (in ha) of patches remaining through 2020 simulated using the three LUCC models and two different scenarios; **b** Coefficient of variation (*CV*) of mean patch area of LUCC simulations

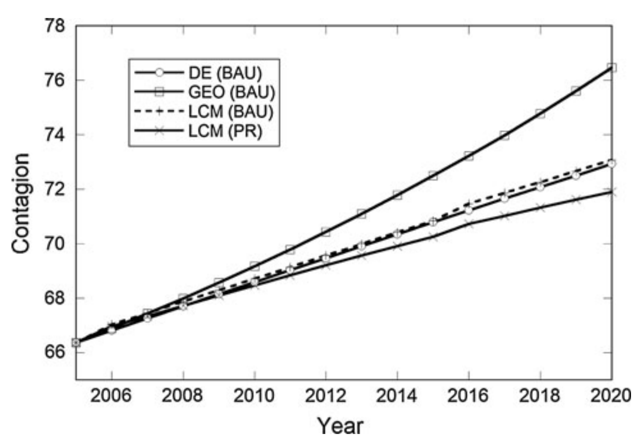


**Fig. 6** The contagion metric, which provides a measure of patch dispersion or clumping, at each time step for the different simulated landscapes calculated with Fragstats. The greater the value, the more clumped or less dispersed the simulated forest patches

yielded a percent agreement of 90.85. Further, the percent agreement was 92.74 for the 2020 LCM and GEOMOD products, indicating that these simulations shared the greatest overall similarity of PSF/non-PSF distribution.

Figures 4, 5, 6, 7 provide different landscape-level metrics with 2005 values obtained from the GoI land cover map. Figure 4 shows very different outcomes among the models with overall negative trends in number of forest patches in the LCM and GEOMOD simulations, but a positive trend in the DE simulation. The GEOMOD simulation also produced the largest interannual variability, whereas the LCM BAU and LCM PR scenarios produced nearly identical time series. Consistent with the relatively high number of patches and positive trend in this metric, the DE projections also produced the smallest mean patch area after 15 years (Fig. 5a). Interestingly, the mean patch area in the LCM BAU projection remained relatively steady from 2008-2020; whereas the LCM PR scenario resulted in a decrease in mean patch area from 2005–2008, followed by a fairly steady increase from 2009–2020 (5,040–6,601 ha, respectively). Landscape-level variation in patch size as indicated by the coefficient of variation (CV) in patch area was high (CV ranged from 600 to 1100 for simulated landscapes) for all models (Fig. 5b) with the models showing an overall decrease in CV through time suggesting that simulated landscapes become more homogeneous, which is consistent with general theory that fragmentation decreases in the latter stages of the tropical deforestation process (Lambin 1997).

Consistent with the maps shown in Fig. 1, dispersion of forest patches as measured by the contagion metric (McGarigal and Marks 1995) for the GEOMOD $3 \times 3$ BAU simulation was the highest and showed a strong, slightly curvilinear positive trend through time (Fig. 6). The contagion metric for the other simulations produced fairly similar values with linear trends ranging from approximately 67 at the beginning of the simulation period to around 72 by 2020. The LCM PR simulation yielded a somewhat more dispersed landscape pattern than the other

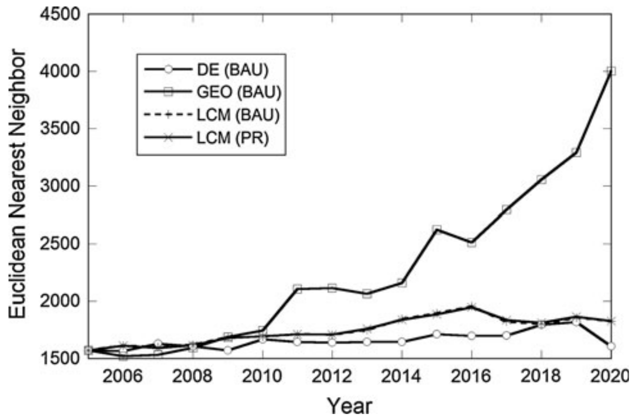


**Fig. 7** Euclidean nearest neighbor (*ENN*) metric, which provides a measure of patch connectivity, calculated through time using Fragstats. The higher the ENN, the more connected the forest patches

simulations even though deforestation was constrained (i.e., not allowed) in Sebangau NP. Consistent with these results, we found that the LCM and DE simulations produced similar Euclidean nearest neighbor (ENN) metrics through time, whereas the GEOMOD BAU scenario produced a time series that diverged strongly from the others, indicating a high level of patch connectivity by 2020 (Fig. 7).

## Discussion and Conclusions

Assessment of our validation runs using the figure of merit (Fig. 2) suggests that the accuracy of our projections is comparable to other studies that have employed LUCC models in a similar fashion. For example, Pontius and others (2008) performed a survey of 13 different land change models and showed that the figure of merit ranged from 1 to 59% with a median value of 21%. Our validations suggest that the most appropriate model to simulate quantity of change for our study area is linear extrapolation; whereas the various LCM configurations may be most appropriate to project the allocation of change. However, it is important to emphasize that any given model may produce an enormous range of different outputs owing to variations of the input parameters. For example, using the Behavioral Landscape Model, an agent-based model, Pontius and others (2007) varied the parameters and produced a wide range of simulations that yielded figures of merit from 27 to 35%, somewhat higher than we found for our study. Thus, the differences between the models as to quantity and allocation of PSF and non-PSF should not be interpreted as a function of the models themselves, but how they were parameterized for these simulations. In our case, the primary interest was to explore change quantity and therefore the GEOMOD simulations may be more appropriate, but as more spatial information becomes available on landscape-level carbon content (e.g., Ruesch and Gibbs 2008), accurate simulation of allocation may become a higher priority and the LCM simulations may provide more meaningful output.

In terms of reducing carbon emissions, our analysis suggests modest carbon emission reductions may result if protection of the Sebangau National Park is effective but produces leakage. A similar study conducted for East Kalimantan (Harris and others 2008) that used GEOMOD projected an additional forest loss of 0.23Mha from East Kalimantan's protected areas by 2013, or the equivalent of 0.305 Gt $CO_2$. Our experience with these LUCC models suggests that linear extrapolation is likely to produce a relatively high estimate of forest loss, but that this estimate is still less than shown in the validation data. We conclude that model simulations that provide robust prediction of allocation may be particularly appropriate if forest and soil carbon are spatially heterogeneous, which is likely under most natural conditions. In addition, inter-model variability indicates that an average from a suite of different LUCC models be used to evaluate the potential deforestation similar to the way that ensemble averages are used in climate models to improve forecasting skill when the forecast range is large (Winter and Nychka 2009).

Relative to recent estimates of deforestation rates in Southeast Asia, our LUCC experiments appear to produce estimates that are comparable or slightly higher than those obtained from region-wide evaluations (Achard and others 2002). For example, the deforestation rate on peatlands in Southeast Asia from 1985–2000 has been estimated conservatively at 1.3%/year, which is about the same deforestation rate (1.4%/year) observed for the lowlands of Sumatra and Kalimantan during 2000–2005 (Hansen and others 2009). However, conversion of peatlands is expected to accelerate in Indonesia, which plans to expand oil palm and timber plantations significantly with 27% of new concessions planned on peatland that makes up approximately 12% of Indonesia's total area (Hooijer and others 2006). A new study by Miettinen and others (2011), suggests that PSF is indeed disappearing at rates much greater than the regional average. Although a reduction in deforestation rates has been observed for Indonesia since 2000, observations from multitemporal satellite imagery reveal a near monotonic increase in forest clearing from 2000–2005, especially in coastal lowland areas dominated by PSF (Hansen and others 2009), which is consistent with our model projections. Our deforestation projection curves are also consistent with one other study (Hooijer and others 2006) that projected regional land use change through 2100 by assuming constant 1985–2000 deforestation rates in Sumatra and Kalimantan. Eventually, of course, PSF deforestation must level off as the amount of forest available for cutting and plantation development begins to decline or increasing marginal costs associated with difficult access discourage further conversion. However, other factors require consideration, such as the relative value of PSF versus non-PSF for economic development or biodiversity (Venter and others 2009, Paoli and others 2010) to determine optimal resource location and strategies to reduce carbon emissions and ensure other co-benefits. Also, our models assume no significant change in Indonesian land use policy and its implementation; a recently pledged two-year moratorium on new concessions for peatland and forest conversion by the Indonesian President (Yashwant 2010) might still prove us wrong.

Overall, our exercise with these three LUCC models and two different scenarios produced a range of different outcomes in terms of total deforested area as well as landscape-level spatial patterns. In general, model divergence in both projected area and spatial patterns became more apparent after 2009, which coincided with the end of the validation period. These results have several implications for both biological conservation and estimating potential carbon emissions. In particular, the LCM PR scenario suggests that protecting 0.54 Mha of PSF will result in a net benefit for reducing forest loss and carbon emissions, but that the benefit at the provincial level is less than the total area of the protected area itself (i.e., only about 0.24 Mha of additional forest remained after 15 years). This suggests that the LCM may simulate leakage effects associated with displacement of deforestation activities in response to a policy intervention (Busch and others 2009). However, leakage is likely to be highly context specific. For example, a recent study by Gaveau and others (2009) using propensity score matching found that protected areas in Sumatra reduced deforestation inside as well as outside those areas. In terms of conservation benefits, the scenario that produces the best outcome would generally be the one that conserves the most forest with the highest connectivity and largest mean patch size. For the BAU scenarios, therefore, the LCM appears to suggest a more favorable conservation outcome overall with the LCM PR scenario suggesting a significant potential benefit in terms of increased patch area, which is a critical parameter for purposes of biological conservation. Generally, Figs. 4, 5, 6, 7 reveal interesting and variable temporal behavior in each model's resulting patch configurations. Whereas we expected to find more monotonic behavior, as in the contagion metric, some metrics such as the mean patch area and number of patches fluctuated and showed somewhat unstable behavior, particularly in the case of the GEOMOD BAU simulation. Further investigation of how these models produce different landscape patterns using standard metrics from Fragstats appears to be warranted if such models are adopted for conservation planning purposes.

Our LUCC modeling study is the first systematic application of proximate driver LUCC models to study deforestation of this critical forest type, and our results suggest the need for more information on the spatial heterogeneity of carbon stocks for PSF in Southeast Asia. One potential limitation of our study is that our LUCC model parameterizations included a major deforestation event associated with the MRP, which was abandoned in 1999 after nearly 80% of the area was severely damaged by the fires of 1997/98 (Page and others 2009) and soils turned out to be poorly suited to agriculture. However, the recent study Miettinen and others (2011) using MODIS 250 m imagery showed that the eastern lowlands of Sumatra and the peatlands of Sarawak, Borneo lost around half of their 2000 PSF cover by 2010. For reasons related to ease of access, low relief and ease of burning during dry periods, PSF in Borneo and Sumatra appears to be under exceptional pressure for plantation development, particularly for oil palm and other plantation crops such as coconuts and acacia. Thus, the MRP, which once appeared to be something of an anomaly, may actually be somewhat typical of the changes that lie ahead for this carbon-rich forest-soil type.

Extending our results to REDD-based policies, accurate carbon emissions projection based on LUCC model scenarios will benefit from consideration of partially degraded forest and peat soils, complete spatial data on peat carbon density and burn depths from extensive LIDAR surveys (Ballhorn and others 2009), inclusion of $CO_2$ uptake to yield net C emissions and accurate estimation of regrowth, reforestation, and plantation development observed from satellite imagery. Furthermore, if only loss and combustion of above-ground PSF biomass are considered, then large uncertainties in carbon stock estimates and deforestation rates suggest that Indonesia may not qualify for carbon credits derived from post-Kyoto climate agreements (Köhl and others 2009). Therefore, inclusion of peatlands in BAU and REDD projections based on LUCC models should become a critical part of Indonesia's strategy to participate in voluntary and future compliance markets as part of a future international REDD mechanism.

**Acknowledgments** The authors thank the editors and the anonymous reviewers for their valuable comments. The Indonesia-Australia Forest Climate Partnership (IACFP) in Jakarta and Central Kalimantan provided data and financial support to MH and DF needed to initiate this research activity.

## References

Achard F, Eva HD, Stibig H-J, Mayaux P, Gallego J, Richards T, Maningreau J-P (2002) Determination of deforestation rates of the world's humid tropical forests. Science 297:999–1002

Ballhorn U, Siegert F, Mason M, Suwido L (2009) Derivation of burn scar depths and estimation of carbon emissions with LIDAR in Indonesian peatlands. Proceedings National Academy of Sciences USA 106:21213–21218

Busch J, Strassburg B, Catteneo A, Lubowski R, Bruner A, Rice R, Creed A, Ashton R, Boltz F (2009) Comparing climate and cost impacts of reference levels for reducing emissions from deforestation. Environmental Research Letters 4:044006

Curran LM, Trigg SN, McDonald AK, Astiani D, Hardiono YM, Siregar P, Caniago I, Kasischke E (2004) Lowland forest loss in protected areas in Indonesian Borneo. Science 303:1000–1003

Deadman P, Robinson D, Moran E, Brondizio E (2004) Colonist household decision making and land-use change in the Amazon Rainforest: an agent-based simulation. Environment and Planning B 31:693–709

Dennis RA, Colfer CP (2006) Impacts of land use and fire on the loss and degradation of lowland forest in 1983–2000 in East Kutai District, East Kalimantan, Indonesia. Singapore Journal of Tropical Geography 27:30–48

Eastman R (2006) Idrisi: The Andes edition. Clark Labs, Worcester

Fuller DO (2003) MODIS data used to study 2002 fires in Kalimantan, Indonesia, vol 84. Eos, Transactions, American Geophysical Union, p 189, 192

Fuller DO (2005) Remote detection of invasive Melaleuca (*Melaleuca quinquenervia*) trees in South Florida with multispectral IKONOS imagery. International Journal of Remote Sensing 26:1057–1063

Fuller DO, Jessup TC, Salim A (2004) Loss of forest cover in Kalimantan, Indonesia since the 1997–1998 El Niño. Conservation Biology 18:249–254

Gaveau DLA, Epting J, Lyne O, Linkie M, Kumara I, Kanninen M, Leader-Williams N (2009) Evaluating whether protected areas reduce tropical deforestation in Sumatra. Journal of Biogeography 36:2165–2175

Geist HJ, Lambin EF (2002) Proximate causes and underlying driving forces of tropical deforestation. Bioscience 52:143–150

Gibbs HK, Brown S, Niles JO, Foley JA (2007) Monitoring and estimating tropical forest carbon stocks: making REDD a reality. Environmental Research Letters 2:045023

Government of Indonesia (2009) Summary for policy makers second National communication under the United Nations Framework Convention on Climate Change and Indonesia Climate Change Accord

Hansen MC, Stehman SV, Potapov PV, Arunarwati B, Stolle F, Pittman K (2009) Quantifying changes in the rates of forest clearing in Indonesia from 1990 to 2005 using remotely sensed data sets. Environmental Research Letters 4. doi:10.1088/1748-9326/4/3/034001

Harris NL, Petrova S, Stolle F, Brown S (2008) Identifying optimal areas for REDD intervention: East Kalimantan, Indonesia as a case study. Environmental Research Letters 3. doi:10.1088/1748-9326/3/3/035006

Hooijer A, Silvius M, Wösten H, Page S (2006) PEAT-CO2, Assessment of CO2 emissions from drained peatlands in SE Asia. Delft Hydraulics report Q3943. http://www.wldelft.nl/cons/area/rbm/PEAT-CO2.pdf. Accessed online 10 June 2010

Jaenicke J, Rieley JO, Mott C, Kimman P, Siegert F (2008) Determination of the amount of carbon stored in Indonesian peatlands. Geoderma 147:151–158

Köhl M, Baldauf T, Plugge D, Krug J (2009) Reduced emissions from deforestation and forest degradation (REDD): a climate change mitigation strategy on a critical track. Carbon Balance and Management 4. doi:10.1186/1750-0680-4-10

Lambin EF (1997) Modelling and monitoring land-cover change processes in tropical regions. Progress in Physical Geography 21:375–393

Langner A, Siegert F (2009) Spatiotemporal fire occurrence in Borneo over a period of 10 years. Global Change Biology 15:48–62

Li X, Hong HS, Bu R, Wen Q, Chang Y, Yuanman H, Li Y (2005) The adequacy of different landscape metrics for various landscape patterns. Pattern Recognition 38:2626–2638

MacKinnon K, Hatta G, Halim H, Mangalik A (1996) The ecology of Kalimantan. Indonesian Borneo Periplus Editions, Singapore

McGarigal K, Marks BJ (1995) FRAGSTATS: spatial pattern analysis program for quantifying landscape structure. USDA Forest Service General Technical Report PNW-351

Miettinen J, Shi C, Liew SC (2011) Deforestation rates in insular Southeast Asia between 2000 and 2010. Global Change Biology. doi: 10.1111/j.1365-2486.2011.02398.x

Murdiyarso D, Lebel L (2007) Local to global perspectives on forest and land fires in Southeast Asia. Mitigation and Adaptation Strategies for Global Change 12:3–11

Obersteiner M, Huettner M, Kraxner F, McCallum I, Kentaro A, Böttcher H, Fritz S, Gusti M, Havlik P, Kindermann G, Rametsteiner E, Reyers B (2009) On fair, effective and efficient REDD mechanism design. Carbon Balance and Management 4:11. doi:10.1186/1750-0680-4-11

Olander LP, Gibbs HK, Steininger M, Swensen JJ, Murray BC (2008) Reference scenarios for deforestation and forest degradation in support of REDD: a review of data and methods. Environmental Research Letters. doi:10.1088/1748-9326/3/2/025011

Page SE, Siegert F, Rieley JO, Boehm HDV, Jaya A, Limin S (2002) The amount of carbon released from peat and forest fires in Indonesia during 1997. Nature 420:61–65

Page S, Hoscilo A, Wosten H, Jauhiainen J, Silvius M, Rieley J, Ritzema H, Tansey K, Graham L, Vasander H, Limin S (2009) Restoration ecology of lowland tropical peatlands in Southeast Asia: Current knowledge and future research directions. Ecosystems 12:888–905

Paoli GD, Wells P L, Meijaard EM, Struebig J, Marshall A J, Obidzinski K, Tan A, Rafiastanto A, Yaap B, Slik JWF, Morel A, Perumal B, Wielaard N, Husson S, and D'Arcy L (2010) Biodiversity Conservation in the REDD Carbon Balance and Management 5:7. doi:10.1186/1750-0680-5-7

Pontius RG, Chen H (2006) GEOMOD modeling. http://www.clarku.edu/~rpontius/. Accessed online 10 June 2010

Pontius RG, Cornell J, Hall CAS (2001) Modeling the spatial pattern of land-use change with GEOMOD2: application and validation for Costa Rica. Agriculture, Ecosystems and Environment 85: 191–203

Pontius RG et al (2007) Accuracy assessment for a simulation model of Amazonian deforestation. Annals of the Association of American Geographers 97:677–695

Pontius RG et al (2008) Comparing the input, output, and validation maps for several models of land change. Annals of Regional Science 42:11–37

Pontius RG, Menon S, Duncan J, Gupta S (2009) Fundamentals for using geographic information science to measure effectiveness of land conservation projects. In: Joshi PK et al (eds) Geoinformatics for Natural Resource Management. Nova Science Publishers, New York, pp 539–557

Ruesch A, Gibbs HK (2008) New IPCC Tier-1 Global Biomass Carbon Map For the Year 2000. Oak Ridge National Laboratory, Oak Ridge, Tennessee. Available online from the Carbon Dioxide Information Analysis Center http://cdiac.ornl.gov

Siegert F, Ruecker G, Hinrichs A, Hoffmann AA (2001) Increased damage from fires in logged forests during droughts caused by El Niño. Nature 412:437–440

Soares-Filho BS, Rodrigues H, Costa W (2009) Modeling Environmental Dynamics with Dinamica EGO. www.csr.ufmg.br/dinamica. Accessed online 8 June 2010 van der Werf GR et al (2008) Climate regulation of fire emissions and deforestation in equatorial Asia. Proceedings of the National Academy of Sciences USA 105:20350–20355

Venter O, Meijaard E, Possingham H, Dennis R (2009) Carbon payments as a safeguard for threatened tropical mammals. Conservation Letters 2:123–129

Whitten AJ, Damanik SJ, Jazanul A, Nazaruddin H (1987) The ecology of Sumatra. Gadjah Mada University Press, Yogyakarta

Winter CL, Nychka D (2009) Forecasting skill of model averages. Stochastic Environmental Research and Risk Assessment 24:633–638

Yashwant S (2010) Fighting for forests. The Jakarta Globe accessed online 10 June 2010 http://www.thejakartaglobe.com/opinion/fighting-for-forests/379290